Environmental Science and Pollution Research (2019) 26:27063–27072
https://doi.org/10.1007/s11356-019-05884-7

RESEARCH ARTICLE

Multi-wavelength spectrophotometric determination of hydrogen peroxide in water by oxidative coloration of ABTS via Fenton reaction

Mengyun Wang[1] · Daiyao Wang[1] · Shiyi Qiu[1] · Junyang Xiao[1] · Huahua Cai[2] · Jing Zou[1]

Received: 12 February 2019 / Accepted: 1 July 2019 / Published online: 17 July 2019

Abstract

In this study, a sensitive and low-cost multi-wavelength spectrophotometric method for the determination of hydrogen peroxide (H_2O_2) in water was established. The method was based on the oxidative coloration of 2,2′-azino-bis(3-ethylbenzothiazoline-6-sulfonate) (ABTS) via Fenton reaction, which resulted in the formation of green radical ($ABTS^{\bullet+}$) with absorbance at four different wavelengths (i.e., 415 nm, 650 nm, 732 nm, and 820 nm). Under the optimized conditions (C_{ABTS} = 2.0 mM, C_{Fe}^{2+} = 1.0 mM, pH = 2.60 ± 0.02, and reaction time (t) = 1 min), the absorbance of the generated $ABTS^{\bullet+}$ at 415 nm, 650 nm, 732 nm, and 820 nm were well linear with H_2O_2 concentrations in the range of 0–40 μM ($R^2 > 0.999$) and the sensitivities of the proposed Fenton-ABTS method were calculated as 4.19×10^4 M^{-1} cm^{-1},1.73×10^4 M^{-1} cm^{-1}, 2.18×10^4 M^{-1} cm^{-1}, and 1.96×10^4 M^{-1} cm^{-1}, respectively. Meanwhile, the detection limits of the Fenton-ABTS method at 415 nm, 650 nm, 732 nm, and 820 nm were respectively calculated to be 0.18 μM, 0.12 μM, 0.10 μM, and 0.11 μM. The absorbance of the generated $ABTS^{\bullet+}$ in ultrapure water, underground water, and reservoir water was quite stable within 30 min. Moreover, the proposed Fenton-ABTS method could be used for monitoring the variations of H_2O_2 concentration during the oxidative decolorization of RhB in alkali-activated H_2O_2 system.

Keywords H_2O_2 · Fe^{2+} · ABTS · Multi-wavelength · Spectrophotometric method · Fenton

Introduction

Hydrogen peroxide (H_2O_2) is a versatile chemical and widely exists in rain, ice, and surface water. The main industrial applications of H_2O_2 are bleaching of textiles and paper (Mounteer et al. 2007). It also plays an important role in Fenton and Fenton-like systems for removing organic pollutants from wastewater (Audino et al. 2018; Koltsakidou et al. 2017). However, H_2O_2 in water can also cause toxic to cells (Aydin et al. 2012). Consequently, there is a necessity for the rapid and accurate detection of H_2O_2 in water.

Until now, there are lots of methods available for the analysis of H_2O_2 concentration in water, including titration (Kieber and Helz 1986; Sully and Williams 1962), electrochemistry (Evans et al. 2002; Jia et al. 2009; Li et al. 2007; Razmi et al. 2010), fluorescence (Li and Townshend 1998; Sakuragawa et al. 1998), chemiluminescence (Hu et al. 2007; Tahirović et al. 2007), and spectrophotometry (Amelin et al. 2000; Hoshino et al. 2014; Sellers 1980; Zhang et al. 2000). As a classical titrimetric method, iodometric titration is usually used to measure H_2O_2 concentration (De Laat and Gallard 1999). Nevertheless, the iodometric method is quite cumbersome and time-consuming due to the titration steps. What's more, due to its high detection limit (DL = 0.02 mM) (Steger and Mühlebach 1997), the iodometric method is unsuitable for the accurate measurement of low concentration of H_2O_2. Although electrochemistry, fluorescence, and chemiluminescence are very sensitive, the expensive apparatuses are required to measure the H_2O_2 concentration (Jia et al. 2009; Sakuragawa et al. 1998; Tahirović et al. 2007), which is not appropriate for routine analysis. Thus, spectrophotometry is considered to be a promising method for H_2O_2 determination due to its easy operation, fast analysis, and low cost.

Responsible editor: Vítor Pais Vilar

✉ Jing Zou
zoujing@hqu.edu.cn; zoujing05@126.com

[1] Institute of Municipal and Environmental Engineering, College of Civil Engineering, Huaqiao University, Xiamen 361021, People's Republic of China

[2] State Key Laboratory of Urban Water Resource and Environment, Harbin Institute of Technology, Harbin 150090, People's Republic of China

Earlier, Bader et al. founded a spectrophotometry in which the colorless *N, N'*-diethyl-*p*-phenylenediamine (DPD) was oxidized by a peroxidase (POD)-catalyzed reaction and generated red-colored $DPD^{\bullet+}$ (Bader et al. 1988). The generated $DPD^{\bullet+}$ had a strong absorbance at 551 nm. However, as shown in Fig. 1a, when the concentration of H_2O_2 was in the range of 0–100 μM, the absorbance of the generated $DPD^{\bullet+}$ solution increased with the increase of H_2O_2 concentration, while then decreased from 100 μM, leading to one absorbance determined at 551 nm matches with two diverse H_2O_2 concentrations. Therefore, in order to accurately measure the H_2O_2 concentration by the POD-DPD method, it is necessary to dilute the water sample containing the high H_2O_2 concentration (Zou et al. 2019a). In addition, when there are some dyes (e.g., acid orange 7, methyl violet and rhodamine B), the absorbance measured by the POD-DPD method will increase significantly because of their strong absorption around 551 nm (Ding et al. 2011).

On this basis, Cai et al. reported a multi-wavelength spectrophotometric method based on a POD-catalyzed reaction where the green-colored $ABTS^{\bullet+}$ was generated from the colorless 2,2′-azino-bis(3-ethylbenzothiazoline-6-sulfonate) (ABTS) (Cai et al. 2018). The generated $ABTS^{\bullet+}$ had four characteristic peaks (i.e., 415 nm, 650 nm, 732 nm, and 820 nm), which could be measured by spectrophotometers. Thus, the POD-ABTS method could avoid the interference of colored coexisting substances, such as dyes. However, when the concentration of H_2O_2 was varying from 0 to 60 μM, the absorbance of the generated $ABTS^{\bullet+}$ solution increased with the increase of H_2O_2 concentration, while then slowly decreased from 60 μM, leading to one absorbance determined at 415 nm matches with two diverse H_2O_2 concentrations, as shown in Fig. 1b. In addition, the enzyme catalyst is too expensive for the routine assay. Besides, Luo et al. established a spectrophotometry to determine the H_2O_2 concentration, which was measured at 464 nm using hydroxyl radical (•OH) generated by Fenton reaction to decolor the methyl orange (MO) (Luo et al. 2008). Although the Fenton-MO method is easy to operate and inexpensive, the persistent dye pollutant is needed, resulting in the hazardous wastewater is produced after the determination of H_2O_2.

To our knowledge, there is not a rapid, sensitive, and low-cost spectrophotometry to detect the H_2O_2 concentration in water using non-toxic analytical reagents. Hence, developing a new method for detecting the H_2O_2 concentration in water is considerable important. Consequently, ABTS, a widely used and environmentally friendly indicator (Cai et al. 2018; Fan et al. 2017; Pinkernell et al. 1997; Pinkernell et al. 2000; Wang and Reckhow 2016; Lee et al. 2005; Zou et al. 2019b), was selected as the probe molecule for the generated •OH from Fe^{2+}-activated H_2O_2 (Fenton reaction) then for the purpose of determination of H_2O_2 concentration. The purposes of this research were establishing a new multi-wavelength spectrophotometry to determine the concentration of H_2O_2 based on the Fenton reaction, optimizing operation parameters (i.e., reaction time, initial solution pH, and the initial concentrations of ABTS and Fe^{2+}), determining the correction curves, investigating the stability of the generated $ABTS^{\bullet+}$, applying the proposed Fenton-ABTS method into the alkali-activated H_2O_2 system monitoring the variation of H_2O_2 concentration during the decolorization of RhB.

Materials and methods

Reagents and solutions

Hydrogen peroxide (H_2O_2, purity 30%), ferrous sulfate heptahydrate ($FeSO_4{\cdot}7H_2O$, AR), rhodamine B (RhB, AR), sodium dihydrogen phosphate dihydrate ($NaH_2PO_4{\cdot}2H_2O$, AR), disodium hydrogen phosphate (Na_2HPO_4, AR), sodium chloride (NaOH, AR), sodium sulfate (Na_2SO_4, AR), sodium bicarbonate ($NaHCO_3$, AR), potassium nitrate (KNO_3, AR), sodium hydroxide (NaOH, AR), and perchloric acid ($HClO_4$,

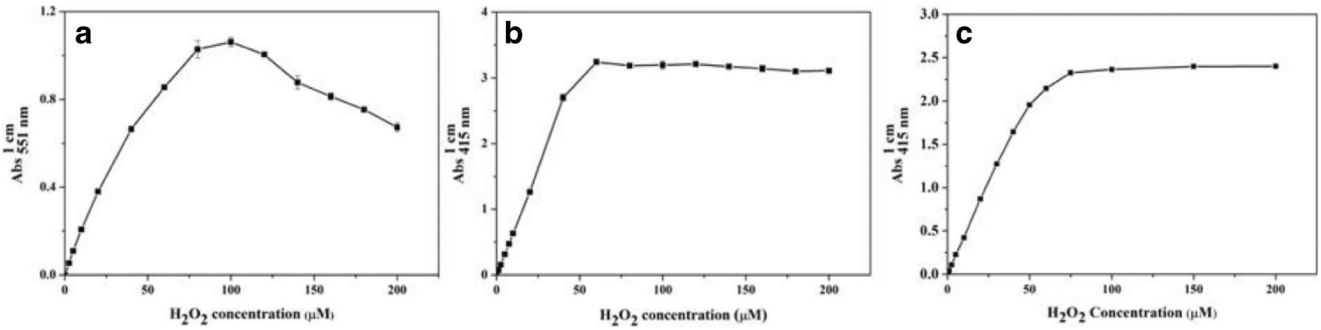

Fig. 1 Three different spectrophotometric methods for the determination of H_2O_2 concentration (0–200 μM). **a** The POD-DPD method. Reaction conditions: $[POD]_0$ = 0.01 mg L^{-1}, $[DPD]_0$ = 0.2 mM, pH = 6.0 (50 mM phosphate buffer), reaction time (t) = 30 s, and T = 24 ± 2 °C. **b** The POD-ABTS method. Reaction conditions: $[POD]_0$ = 0.01 mg L^{-1}, $[ABTS]_0$ = 0.1 mM, pH = 6.0 (50 mM phosphate buffer), t = 30 s, and T = 24 ± 2 °C. **c** The Fenton-ABTS method. Reaction conditions: $[ABTS]_0$ = 2.0 mM, $[Fe^{2+}]_0$ = 1.0 mM, pH = 2.60 ± 0.02, t = 1 min, and T = 24 ± 2 °C. Error bars represent the standard deviations of duplicate measurements

AR) were purchased from Sinopharm Chemical Reagent Co., Ltd (Shanghai, China). DPD (purity 98%), humic acid (purity 90%), ABTS (purity 98%), and POD (specific activity of 200 units mg^{-1}) were purchased from Aladdin Bio-Chem Technology Co., Ltd (Shanghai, China).

The ABTS solution (10 mM) was freshly prepared by dissolving 0.1400 g of ABTS into 25 mL of ultrapure water. H_2O_2 concentration in 30% H_2O_2 solution was firstly titrated as 9.76 M with standard $KMnO_4$ solution. H_2O_2 working solution (0.5 mM) was prepared from 30% H_2O_2 solution and stored under dark condition. POD solution (0.5 g L^{-1}) and DPD solution (5 mM) were stored under dark condition and changed once a week. All the above solutions needed to be stored at 4 °C. $FeSO_4$ solution (10 mM) was freshly prepared by dissolving 0.0695 g $FeSO_4{\cdot}7H_2O$ into 25 mL of ultrapure water. RhB solution (5 mM) was prepared by dissolving 0.1198 g of RhB into 50 mL of ultrapure water. 50 mM of phosphate buffers with pH 6.0 was prepared with NaH_2PO_4 solution (50 mM) and Na_2HPO_4 solution (50 mM). Throughout the experiments, the stock solutions of $HClO_4$ and NaOH were employed for pH adjustment.

Experimental apparatus

The absorbance value in this study was recorded by a spectrophotometer (Persee TU-1901, China). The pH measurements and electrical conductivity were carried out with a PB-10 pH-meter (Sartorius, Germany). Dissolved organic carbon (DOC) and inorganic carbon (IC) were measured with a total organic carbon analyzer (TOC-V, Shimadzu, Japan). Concentrations of Cl^-, NO_3^-, and SO_4^{2-} were determined with an ion chromatography (930 Compact IC, China). Ultrapure water used in this study (18.2 MΩ cm) was produced with a laboratory ultrapure water system (Shanghai Hetai Instruments Co. Ltd, China).

Natural waters

Two different natural waters were adopted to evaluate the proposed Fenton-ABTS method: (1) Underground water sample collected from an industrial drinking water treatment plant in Longyan City (pH = 7.62, Electrical conductivity = 31.60 mV, DOC = 3.67 mg L^{-1}, IC = 47.19 mg L^{-1}, Total hardness = 230.58 mg L^{-1} as $CaCO_3$, Cl^- concentration = 35.59 mg/L, NO_3^- concentration = 25.40 mg/L, and SO_4^{2-} concentration = 75.34 mg/L,); (2) Reservoir water sample collected from Lianban reservoir in Xiamen City (pH = 7.83, Electrical conductivity = 42.20 mV, DOC = 5.36 mg L^{-1}, IC = 6.65 mg L^{-1}, Total hardness = 49.85 mg L^{-1} as $CaCO_3$, Cl^- concentration = 21.39 mg/L, NO_3^- concentration = 7.51 mg/L, and SO_4^{2-} concentration = 12.81 mg/L,). The natural water samples were filtered through 0.45 μm cellulose acetate membranes before the experiments and then stored at 4 °C.

Experimental procedures

General steps for determining H_2O_2 concentration in water samples with the Fenton-ABTS method were described as Scheme 1. The steps for determination of H_2O_2 concentration by the POD-DPD method and the POD-ABTS method were performed as reported earlier (Bader et al. 1988; Cai et al. 2018) (Scheme 1).

The steps for measuring the change of RhB concentration in alkali-activated hydrogen peroxide system were as follows: at the predetermined interval time, 1.2 mL of reaction solution was transferred into 1 cm quartz cell which had contained 1.3 mL of $HClO_4$ stock solution (1.0 M) to suspend the reaction. Then, the change in absorbance from 200 to 800 nm was obtained by the UV-Vis spectrophotometer.

Thus, the H_2O_2 concentration in water was calculated from the measured absorbance change of $ABTS^{\bullet+}$ at 415 nm, 650 nm, 732 nm, or 820 nm by following relationship:

$$[H_2O_2]_{sample} = \frac{\gamma \Delta A_l V_{final}}{\varepsilon l V_{sample}}$$

where

ΔA_l = absorbance at four characteristic wavelengths

l = path length of quartz cell

γ = stoichiometric factor of $ABTS^{\bullet+}$ generation (0.80, refer to the "Effect of reaction time" section for further details)

ε = molar absorptivity of $ABTS^{\bullet+}$

V_{final} = final volume of reaction solutions

V_{sample} = volume of original H_2O_2 samples

The molar absorptivity of $ABTS^{\bullet+}$ at four characteristic wavelengths were determined at pH 2.60 by using NaClO and ABTS to produce $ABTS^{\bullet+}$ in the presence of iodide (6 μM) as a catalyst. According to previous reports, 1 mol of NaClO and 2 mol of ABTS could generate 2 mol of $ABTS^{\bullet+}$ (Pinkernell et al. 2000; Lee et al. 2005). With this method, the molar absorptivity of $ABTS^{\bullet+}$ at these four characteristic wavelengths were respectively obtained to be 3.37×10^4 M^{-1} cm^{-1}, 1.38×10^4 M^{-1} cm^{-1}, 1.74×10^4 M^{-1} cm^{-1}, and 1.55×10^4 M^{-1} cm^{-1}. The calculated molar absorptivity of $ABTS^{\bullet+}$ at 415 nm was consistent with other reports (Cai et al. 2018; Fan et al. 2017; Tao and Reckhow 2016), while the other three molar absorptivity of $ABTS^{\bullet+}$ were higher than that at pH 6.0 reported by Cai et al., where the molar absorptivity of $ABTS^{\bullet+}$ were respectively reported to be 0.98×10^4 M^{-1} cm^{-1}, 1.33×10^4 M^{-1} cm^{-1}, and 1.04×10^4 M^{-1} cm^{-1} at 650 nm, 732 nm, and 820 nm (Cai et al. 2018). The cause of this phenomenon might be the difference in solution pH.

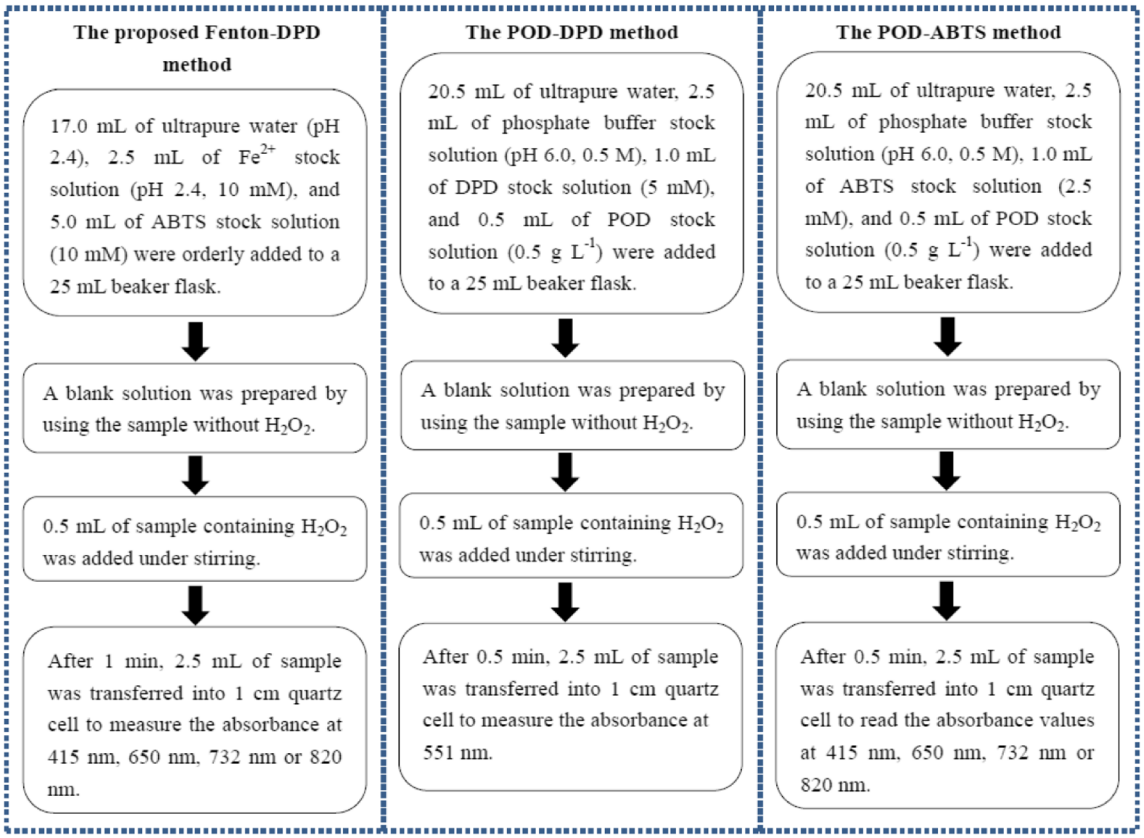

Scheme 1 Flowchart showing the analysis steps of the proposed Fenton-DPD method, the POD-DPD method, and the POD-ABTS method

Results and discussion

Absorption spectra of $ABTS^{\bullet+}$

Figure 2 shows the absorption spectra of the generated $ABTS^{\bullet+}$ in Fenton-ABTS system. As could be seen, there were four easily distinguished peaks (i.e., 415 nm, 650 nm, 732 nm, and 820 nm) in the absorption spectra of $ABTS^{\bullet+}$, which was identical to other literatures (Fan et al. 2017; Ma et al. 2009; Pinkernell et al. 1997). As shown in Fig. 2, the measured absorbance increased with the increase of H_2O_2 concentration, while the H_2O_2 concentration showed no effect on the shape of the absorption curve and positions of these four characteristic peaks. The correlations between the H_2O_2 concentration and the absorbance of $ABTS^{\bullet+}$ at four characteristic wavelengths provide the possibility for developing a multi-wavelength spectrophotometric method for H_2O_2 determination.

Effects of operation parameters on the determination of H_2O_2

To develop the multi-wavelength spectrophotometric method for detecting the concentration of H_2O_2 in water based on the Fenton oxidation of ABTS, investigating the effects of operation parameters (i.e., reaction time, initial solution pH, and the initial concentrations of ABTS and Fe^{2+}) is of great significance.

Effect of reaction time

Figure 3a shows the influence of reaction time in Fenton-ABTS system, which is represented by absorbance change ΔA ($\Delta A = A_0 - A_t$, where A_0 and A_t are the absorbance of the ABTS solution at

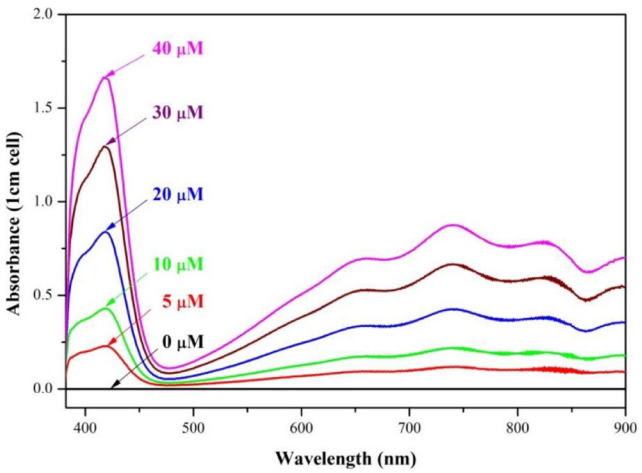

Fig. 2 Absorption spectrum of the generated $ABTS^{\bullet+}$ in Fenton-ABTS system. Reaction conditions: $[H_2O_2]_0$ = 0–40 μM, $[ABTS]_0$ = 2.0 mM, $[Fe^{2+}]_0$ = 1.0 mM, pH = 2.60 ± 0.02, t = 1 min, and T = 24 ± 2 °C

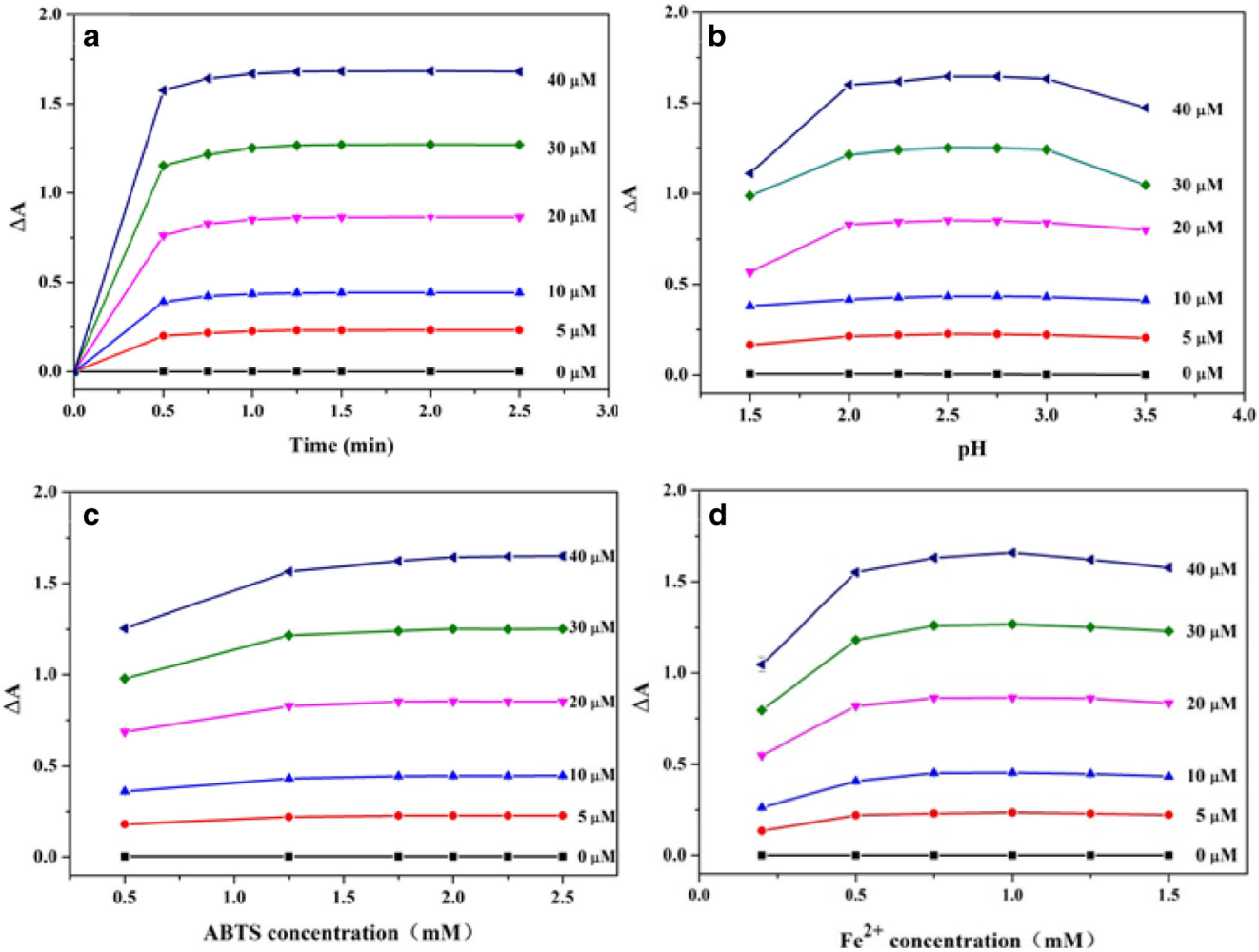

Fig. 3 Effects of reaction time (**a**), initial pH (**b**), initial ABTS concentration (**c**), and initial Fe^{2+} concentration (**d**) on the coloration extent of ABTS at 415 nm in Fenton-ABTS system. Reaction conditions: $[ABTS]_0$ = 2.0 mM for (**a**), (**b**), and (**d**); $[Fe^{2+}]_0$ = 1.0 mM for (**a**), (**b**), and (**c**); $pH_0 = 2.60 \pm 0.02$ for (**a**), (**c**), and (**d**); t = 1 min for (**b**), (**c**) and (**d**); and $T = 24 \pm 2$ °C. Error bars represent the standard deviations of duplicate measurements

415 nm before and after the reaction). ΔA increased quickly with the increase of reaction time initially, and then remained almost unchanged beyond 1 min for each given concentration of H_2O_2 in the range of 0–40 μM. The occurrence of the plateau could be attributed to the complete decomposition of H_2O_2 by the excess of Fe^{2+} in Fenton-ABTS system. Therefore, in our further experiments, reaction time of t = 1 min was chosen as the optimum reaction time for the measurement of H_2O_2.

Effect of initial solution pH

In Fenton-ABTS system, solution pH is a crucial element. According to previous reports, the optimal pH for Fenton oxidation is near pH 3.0 (Pignatello et al. 2006). The precipitation of Fe^{3+} as ferric hydroxide is the major cause for the lower reactivity at higher pH (pH > 4.0), which inhibits the recycling of Fe^{2+} and Fe^{3+} (Georgi et al. 2007). For the sake of optimizing solution pH in Fenton-ABTS system, the effect of solution pH ranging from 1.5 to 3.5 on the coloration extent of ABTS was investigated. As Fig. 3b shows, at pH 1.5–2.0, ΔA increases with increasing pH, stabilizes at pH 2.0–3.0, and then gradually decreases beyond pH 3.0. Thus, pH 2.6 was chosen as the optimum initial solution pH to measure the H_2O_2 concentration in the present work.

Effect of initial ABTS concentration

Figure 3c illustrates the effect of initial ABTS concentration on the coloration extent of ABTS. Initially, ΔA increased with the increasing initial ABTS concentration, and then kept nearly unchanged beyond 2.0 mM ABTS for a given H_2O_2 concentration. Labrinea et al. have reported that $ABTS^{\bullet+}$ is more stable in the presence of excess ABTS, because excess ABTS will inhibit the disproportionation of $ABTS^{\bullet+}$ to produce 1 ABTS and azo salt under acidic pH conditions (Childs and Bardsley 1975; Labrinea and Georgiou 2004). Since our

experiment was carried out under the acidic condition of pH 2.60, a slight excess ABTS was enough to achieve the purpose of stabilizing $ABTS^{\bullet+}$. Consequently, 2.0 mM ABTS was selected for further experiments.

Effect of initial Fe^{2+} concentration

In Fenton systems, in order to avoid the formation of a large amount of iron sludge, it is common to use Fe^{2+} in lower concentrations (Gomez-Herrero et al. 2018). Besides, as the concentration of Fe^{2+} increases, the scavenging effect of Fe^{2+} on •OH increases rapidly. So, it is of great significance to optimize the initial Fe^{2+} concentration in Fenton-ABTS system. The influence of the concentration of Fe^{2+} on the H_2O_2 measurement is shown in Fig. 3d. For each of the given H_2O_2 concentration, ΔA increased initially along with Fe^{2+} concentration in the range of 0.2–1.5 mM, then gradually decreased as Fe^{2+} concentration was beyond 1 mM. Thus, the initial Fe^{2+} concentration was chosen as 1 mM for further experiments.

Correction curves for H_2O_2 determination

As shown in Fig. 4, under the optimized conditions (C_{ABTS} = 2.0 mM, $C_{Fe}{}^{2+}$ = 1.0 mM, pH = 2.60 ± 0.02, and t = 1 min), the correction curves measured for H_2O_2 concentration ranging between 0 and 40 μM at four characteristic wavelengths were well linear ($R^2 > 0.999$) and their slopes (k) at these four characteristic wavelengths were respectively calculated as high as 4.19×10^4 M^{-1} cm^{-1}, 1.73×10^4 M^{-1} cm^{-1}, 2.18×10^4 M^{-1} cm^{-1}, and 1.96×10^4 M^{-1} cm^{-1}. Therefore, it provides the choice of analytical wavelength. Meanwhile, the detection limits (DL = $3\sigma/k$, where σ represents the standard deviation of the blank samples (Luo et al. 2008)) of the proposed Fenton-ABTS method were respectively calculated to be 0.18 μM, 0.12 μM, 0.10 μM, and 0.11 μM at 415 nm, 650 nm, 732 nm, and 820 nm, which suggests that the proposed method has high sensitivity. The stoichiometric factor of the generated $ABTS^{\bullet+}$ ($\gamma = \Delta[H_2O_2]/\Delta[ABTS^{\bullet+}]$) was calculated by dividing the molar absorptivity of $ABTS^{\bullet+}$ ($\varepsilon = \Delta A/\Delta[ABTS^{\bullet+}]$, which has been calculated in the "Experimental procedures" section) by the slope of the calibration curve ($k = \Delta A/\Delta[H_2O_2]$). Hence, the stoichiometric factors of $ABTS^{\bullet+}$ at four characteristic wavelengths were all calculated to be 0.80 ± 0.01. Interestingly, the calculated stoichiometric factor of the generated $ABTS^{\bullet+}$ in Fenton-ABTS system was lower than 1. The phenomenon might be rationally interpreted by the fact that Fe^{3+} produced in Fenton-ABTS system would further react with the ABTS reagent to generate $ABTS^{\bullet+}$.

Furthermore, the correction curves of four characteristic wavelengths for analyzing H_2O_2 in two types of practical samples (underground water and reservoir water) by the proposed Fenton-ABTS method were established. There were also well relationships between the H_2O_2 concentration and the coloration extent of ABTS, and the corresponding slopes of the calibration curves in underground water and reservoir water were nearly the same as that obtained in ultrapure water, as shown in Fig. 5. These results indicate that the proposed Fenton-ABTS method will not be greatly affected by the coexisting substances in natural waters. Furthermore, the experiments of recovery rate in ultrapure water, underground water, and reservoir water by the proposed Fenton-ABTS method were carried out. It was found that the recovery rates of H_2O_2 concentration spiked in these three water samples were all within (100 ± 5.00) % (Table 1).

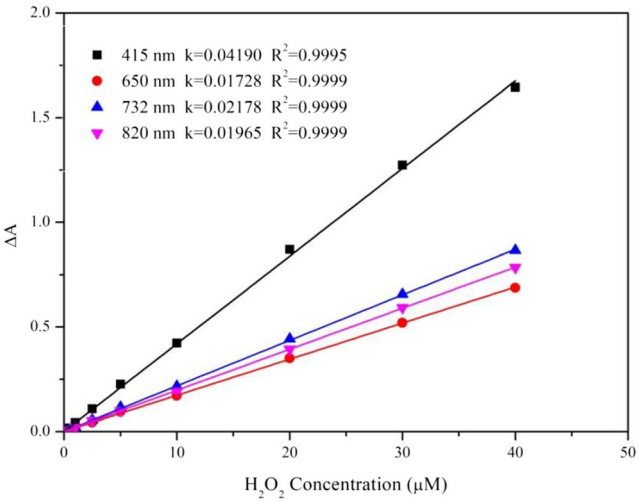

Fig. 4 Correction curves of the Fenton-ABTS method for the measurement of H_2O_2 concentration in ultrapure water. Reaction conditions: $[ABTS]_0$ = 2.0 mM, $[Fe^{2+}]_0$ = 1.0 mM, pH = 2.60 ± 0.02, t = 1 min, and T = 24 ± 2 °C. Error bars represent the standard deviations of six measurements

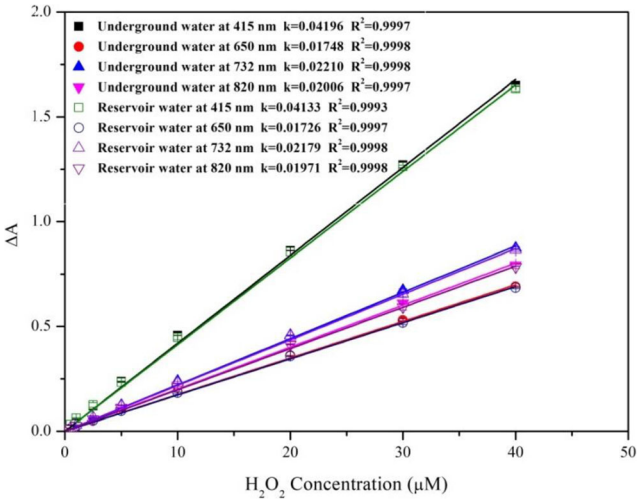

Fig. 5 Correction curves of the Fenton-ABTS method for the measurement of H_2O_2 concentration in underground water and reservoir water. Reaction conditions: $[ABTS]_0$ = 2.0 mM, $[Fe^{2+}]_0$ = 1.0 mM, pH = 2.60 ± 0.02, t = 1 min, and T = 24 ± 2 °C. Error bars represent the standard deviations of six measurements

Table 1 Recovery rate of H_2O_2 concentration with the proposed Fenton-ABTS method (n = 7)

Water samples	Spiked H_2O_2 concentration (μM)	Measured wavelength (nm)	Measured H_2O_2 concentration (μM)	Recovery rate (%)
Ultrapure water	2.19	415	2.25 ± 0.05	102.60
		650	2.23 ± 0.05	101.92
		732	2.28 ± 0.03	104.23
		820	2.28 ± 0.05	104.24
	20.42	415	20.70 ± 0.17	101.37
		650	21.00 ± 0.10	102.38
		732	21.15 ± 0.10	103.59
		820	21.35 ± 0.09	104.57
Underground water	2.19	415	2.26 ± 0.10	103.32
		650	2.20 ± 0.09	100.61
		732	2.20 ± 0.11	100.47
		820	2.21 ± 0.11	101.03
	20.42	415	20.33 ± 0.16	99.54
		650	20.42 ± 0.09	99.98
		732	20.55 ± 0.08	100.65
		820	20.58 ± 0.09	100.77
Reservoir water	2.19	415	2.18 ± 0.07	99.67
		650	2.21 ± 0.09	100.88
		732	2.25 ± 0.09	102.67
		820	2.24 ± 0.08	102.25
	20.42	415	20.25 ± 0.16	99.17
		650	20.34 ± 0.10	99.63
		732	20.47 ± 0.10	100.25
		820	20.56 ± 0.07	100.67

The influences of common coexisting foreign species on the determination of H_2O_2 by the proposed Fenton-ABTS method under the optimized reaction conditions ($[ABTS]_0$ = 2.0 mM, $[Fe^{2+}]_0$ = 1.0 mM, pH = 2.60 ± 0.02, t = 1 min, and T = 24 ± 2 °C) were studied, which was shown in Fig. 6. The relative error for the determination of 25 μM H_2O_2 was no higher than 5% with the existence of 10 mM $NaHCO_3$, 20 mM NaCl, 1 mM Na_2SO_4, 2 mM KNO_3, or 5 mg L^{-1} humic acid, which indicates that the proposed Fenton-ABTS method well effective to tolerate the interferences of common coexisting foreign species in aqueous solutions.

Interestingly, when detecting the H_2O_2 concentration in the range of 0–200 μM with the proposed Fenton-ABTS method, the measured absorbance increased continuously with H_2O_2 concentration (Fig. 1c), implying that one absorbance obtained at 415 nm matches with one specific H_2O_2 concentration. Nevertheless, as shown in Fig. 1a, b, the absorbance of the generated $DPD^{\bullet+}$/$ABTS^{\bullet+}$ solution initially increased with H_2O_2 concentration and then decreased, when the POD-DPD method and the POD-ABTS method were employed for detecting the H_2O_2 concentration in the range of 0–200 μM. In this respect, our proposed Fenton-ABTS method is superior to both of the POD-DPD method and the POD-ABTS method previously reported.

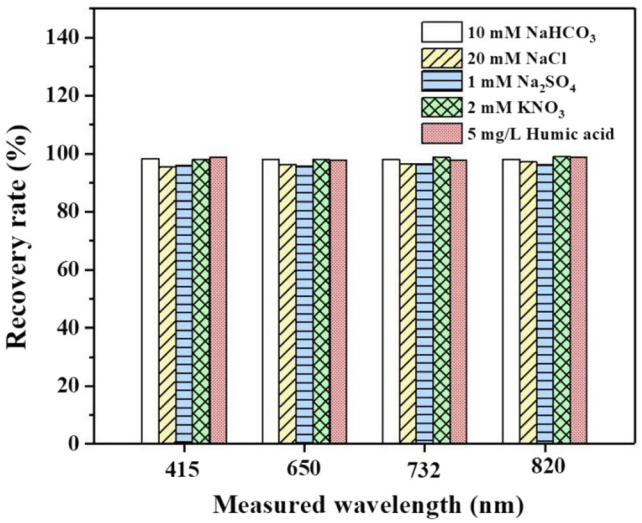

Fig. 6 The influences of common coexisting foreign species on the determination of H_2O_2 by the proposed Fenton-ABTS method. Reaction conditions: $[ABTS]_0$ = 2.0 mM, $[Fe^{2+}]_0$ = 1.0 mM, $[H_2O_2]_0$ = 25 μM, pH = 2.60 ± 0.02, t = 1 min, and T = 24 ± 2 °C. Error bars represent the standard deviations of three measurements

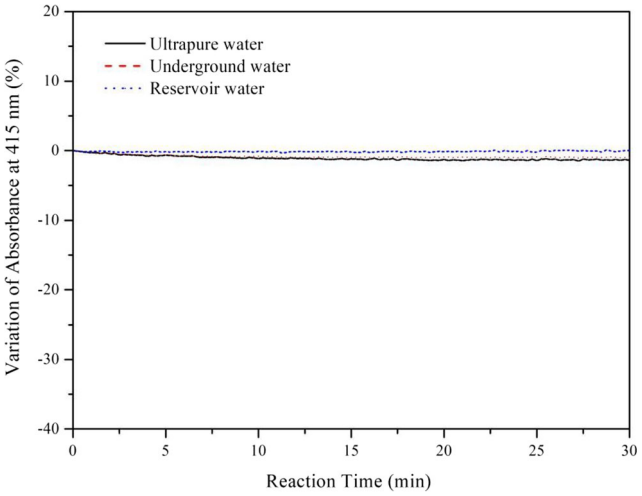

Fig. 7 Stability of $ABTS^{\bullet+}$ generated by Fenton oxidation of ABTS in ultrapure water and natural waters. Reaction conditions: $[ABTS]_0$ = 2.0 mM, $[Fe^{2+}]_0$ = 1.0 mM, pH = 2.60 ± 0.02, t = 1 min, and T = 24 ± 2 °C

Stability of the generated $ABTS^{\bullet+}$

In order to assess the stability of $ABTS^{\bullet+}$ generated in Fenton-ABTS system, the absorbance change of the $ABTS^{\bullet+}$ in ultrapure water, underground water, and reservoir water was measured at 415 nm, as shown in Fig. 7. The absorbance of $ABTS^{\bullet+}$ in these three water samples was quite stable and decreased 0.83%, 1.03%, and 0.00% within 0.5 h, respectively. Therefore, it had enough time to accurately measure the concentration of H_2O_2 in natural waters and ultrapure water using the proposed Fenton-ABTS method. However, it should be noted that the proposed Fenton-ABTS method might be unsuitable for detecting the H_2O_2 concentration in aqueous samples which contain strong reducing substances, because of the antioxidant activity of the generated $ABTS^{\bullet+}$ (Lee et al. 2014; Re et al. 1999; Song et al. 2015; Gu et al. 2019).

Variation of H_2O_2 concentration in alkali-activated H_2O_2 system

The alkali-activated H_2O_2 system had been widely employed for the treatment of dyeing wastewater (Li et al. 2018; Long et al. 2012; Wang et al. 2018). The inset in Fig. 8 showed the decolorization of RhB by alkali-activated H_2O_2. It was found that the strong absorption of RhB near 551 nm was gradually decreased within 120 min. Meanwhile, the proposed Fenton-ABTS method and the previously reported POD-ABTS method were used to monitor the variation of H_2O_2 concentration during the decolorization of RhB in alkali-activated H_2O_2 system, as shown in Fig. 8. As could be seen, H_2O_2 was gradually decomposed over time, and the variation of H_2O_2 concentration monitored with the proposed Fenton-ABTS method was well consistent with that measured by the previously reported POD-ABTS method. These results further suggested that the Fenton-ABTS method proposed in this study was highly accurate for the determination of H_2O_2 concentration. Meanwhile, the proposed Fenton-ABTS method might be superior to the previously reported POD-ABTS method for the routine analysis because Fe^{2+} was much cheaper than POD. Additionally, it should be noted that the traditional POD-DPD method should be unsuitable to measure the H_2O_2 concentration when water samples have strong absorption near 551 nm.

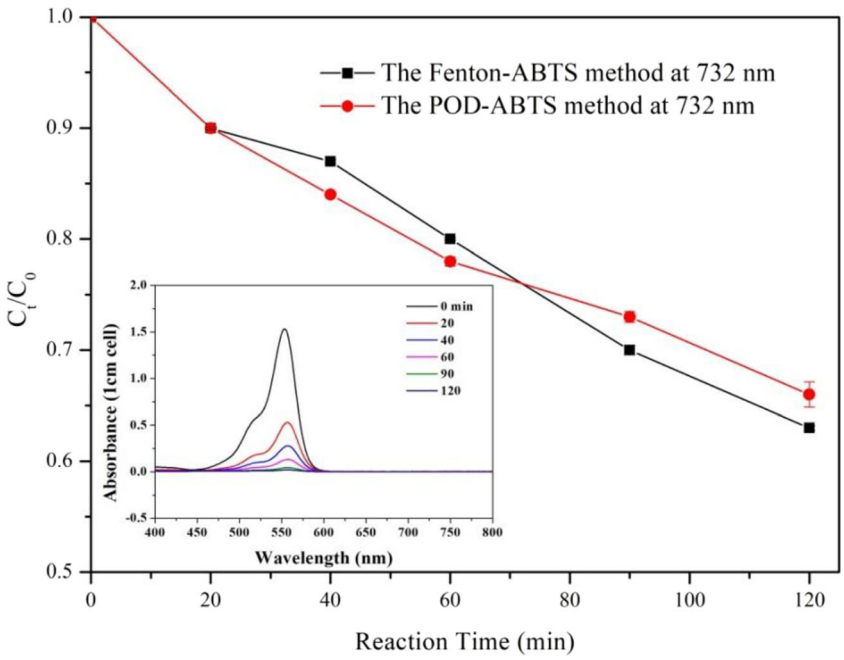

Fig. 8 Variations of H_2O_2 concentration during the oxidative decolorization of RhB in alkali-activated H_2O_2 system. Reaction conditions: $[H_2O_2]_0$ = 36 mM, $[RhB]_0$ = 0.2 mM, and pH $_0$ = 11.50. Error bars represent the standard deviations of duplicate measurements. The inset shows the decolorization of RhB over time

Conclusions

A new multi-wavelength spectrophotometric method was presented. This method depended on the oxidative coloration of ABTS via Fenton reaction. The major features of the proposed Fenton-ABTS method were as follows:

a. Without tedious titrimetric procedures and expensive materials, the proposed Fenton-ABTS method was fast to detect the H_2O_2 concentration within 1 min. This method was quite sensitive (4.19×10^4 M^{-1} cm^{-1} at 415 nm) and the detection limit was as low as 0.18 μM.
b. The product $ABTS^{\bullet+}$ was very stable which permits enough time to accurately measure the H_2O_2 concentration in water.
c. The Fenton-ABTS method well monitored the variation of H_2O_2 concentration during the oxidative decolorization of RhB by alkali-activated H_2O_2.

Funding information This research was supported by the National Natural Science Foundation of China (No. 51708231), China Postdoctoral Science Foundation (No. 2017M612120), Natural Science Foundation of Fujian province (No. 14185013), and Promotion Program for Young and Middle-aged Teacher in Science and Technology Research of Huaqiao University (No. ZQN-YX506).

References

Amelin VG, Kolodkin IS, Irinina YA (2000) Test method for the determination of hydrogen peroxide in atmospheric precipitation and water using indicator papers. J Anal Chem 55:374–377

Audino F, Conte LO, Schenone AV, Pérez-Moya M, Graells M, Alfano OM (2018) A kinetic study for the Fenton and photo-Fenton paracetamol degradation in an annular photoreactor. Environ Sci Pollut Res 26:4312–4323

Aydin Z, Wei Y, Guo M (2012) A highly selective Rhodamine based turn-on optical sensor for Fe^{3+}. Inorg Chem Commun 20:93–96

Bader H, Sturzenegger V, Hoigné J (1988) Photometric method for the determination of low concentrations of hydrogen peroxide by the peroxidase catalyzed oxidation of N,N-diethyl-p -phenylenediamine (DPD). Water Res 22:1109–1115

Cai H, Liu X, Zou J, Xiao J, Yuan B, Li F, Cheng Q (2018) Multi-wavelength spectrophotometric determination of hydrogen peroxide in water with peroxidase-catalyzed oxidation of ABTS. Chemosphere 193:833–839

Childs RE, Bardsley WG (1975) Time-dependent inhibition of enzymes by active-site-directed reagents. A theoretical treatment of the kinetics of affinity labelling. J Theor Biol 53:381–394

De Laat J, Gallard H (1999) Catalytic decomposition of hydrogen peroxide by Fe(III) in homogeneous aqueous solution: mechanism and kinetic modeling. Environ Sci Technol 33:2726–2732

Ding Y, Zhu L, Yan J, Xiang Q, Tang H (2011) Spectrophotometric determination of persulfate by oxidative decolorization of azo dyes for wastewater treatment. J Environ Monit 13:357–363

Evans SAG, Elliott JM, Andrews LM, Bartlett PN, Doyle PJ, Guy D (2002) Detection of hydrogen peroxide at mesoporous platinum microelectrodes. Anal Chem 74:1322–1326

Fan W, Qiao J, Guan X (2017) Multi-wavelength spectrophotometric determination of Cr (VI) in water with ABTS. Chemosphere 171: 460–467

Georgi A, Schierz A, Trommler U, Horwitz CP, Collins TJ, Kopinke FD (2007) Humic acid modified Fenton reagent for enhancement of the working pH range. Appl Catal B-Environ 72:26–36

Gomez-Herrero E, Tobajas M, Polo A, Rodriguez JJ, Mohedano AF (2018) Removal of imidazolium- and pyridinium-based ionic liquids by Fenton oxidation. Environ Sci Pollut Res 25:34930–34937

Gu Y, Xue P, Jia F, Shi K (2019) Co-immobilization of laccase and ABTS onto novel dual-functionalized cellulose beads for highly improved biodegradation of indole. J Hazard Mater 365:118–124

Hoshino M, Kamino S, Doi M, Takada S, Mitani S, Yanagihara R, Asano M, Yamaguchi T, Fujita Y (2014) Spectrophotometric determination of hydrogen peroxide with osmium(VIII) and m-carboxyphenylfluorone. Spectrochim Acta A 117:814–816

Hu Y, Zhang Z, Yang C (2007) The determination of hydrogen peroxide generated from cigarette smoke with an ultrasensitive and highly selective chemiluminescence method. Anal Chim Acta 601:95–100

Jia W, Min G, Zhe Z, Yu T, Rodriguez EG, Ying W, Lei Y (2009) Electrocatalytic oxidation and reduction of H_2O_2 on vertically aligned Co_3O_4 nanowalls electrode: toward H_2O_2 detection. J Electroanal Chem 625:27–32

Kieber RJ, Helz GR (1986) Two-method verification of hydrogen peroxide determinations in natural waters. Anal Chem 58:1944–1945

Koltsakidou A, Antonopoulou M, Sykiotou M, E E KI, Lambropoulou DA (2017) Photo-Fenton and Fenton-like processes for the treatment of the antineoplastic drug 5-fluorouracil under simulated solar radiation. Environ Sci Pollut Res 24:4791–4800

Labrinea EP, Georgiou CA (2004) Stopped-flow method for assessment of pH and timing effect on the ABTS total antioxidant capacity assay. Anal Chim Acta 526:63–68

Lee Y, Yoon J, Von GU (2005) Spectrophotometric determination of ferrate (Fe(VI)) in water by ABTS. Water Res 39:1946–1953

Lee Y, Kissner R, Von GU (2014) Reaction of ferrate(VI) with ABTS and self-decay of ferrate(VI): kinetics and mechanisms. Environ Sci Technol 48:5154–5162

Li YZ, Townshend A (1998) Evaluation of the adsorptive immobilisation of horseradish peroxidase on PTFE tubing in flow systems for hydrogen peroxide determination using fluorescence detection. Anal Chim Acta 359:149–156

Li Z, Cui X, Zheng J, Wang Q, Lin Y (2007) Effects of microstructure of carbon nanofibers for amperometric detection of hydrogen peroxide. Anal Chim Acta 597:238–244

Li Y, Li L, Chen Z, Zhang J, Gong L, Wang Y, Zhao H, Mu Y (2018) Carbonate-activated hydrogen peroxide oxidation process for azo dye decolorization: process, kinetics, and mechanisms. Chemosphere 192:372–378

Long X, Yang Z, Wang H, Chen M, Peng K, Zeng Q, Xu A (2012) Selective degradation of orange II with the cobalt(II)–bicarbonate–hydrogen peroxide system. Ind Eng Chem Res 51:11998–12003

Luo W, Abbas ME, Zhu L, Deng K, Tang H (2008) Rapid quantitative determination of hydrogen peroxide by oxidation decolorization of methyl orange using a Fenton reaction system. Anal Chim Acta 629: 1–5

Ma J, Yang J, Zhao J (2009) Spectrophotometric determination of trace $KMnO_4$ in water with 2,2′-azino-bis(3-ethylbenzothiazoline-6-sulfonate). Acta Sci Circumst 29:668–672

Mounteer AH, Pereira RO, Morais AA, Ruas DB, Silveira DS, Viana DB, Medeiros RC (2007) Advanced oxidation of bleached eucalypt kraft pulp mill effluent. Water Sci Technol 55:109–116

Pignatello JJ, Oliveros E, Mackay A (2006) Advanced oxidation processes for organic contaminant destruction based on the Fenton reaction and related chemistry. Environ Sci Technol 36:1–84

Pinkernell U, Lüke HJ, Karst U (1997) Selective photometric determination of peroxycarboxylic acids in the presence of hydrogen peroxide. Analyst 122:567–571

Pinkernell U, Nowack B, Gallard H, Gunten UV (2000) Methods for the photometric determination of reactive bromine and chlorine species with ABTS. Water Res 34:4343–4350

Razmi H, Mohammad-Rezaei R, Heidari H (2010) Self-assembled prussian blue nanoparticles based electrochemical sensor for high sensitive determination of H_2O_2 in acidic media. Electroanal 21:2355–2362

Re R, Pellegrini N, Proteggente A, Pannala A, Yang M, Riceevans C (1999) Antioxidant activity applying an improved ABTS radical cation decolorization assay. Free Radic Biol Med 26:1231–1237

Sakuragawa A, Tanial T, Okutani T (1998) Fluorometric determination of microamounts of hydrogen peroxide with an immobilized enzyme prepared by coupling horseradish peroxidase to chitosan beads. Anal Chim Acta 374:191–200

Sellers RM (1980) Spectrophotometric determination of hydrogen peroxide using potassium titanium (IV) oxalate. Analyst 105:950–954

Song Y, Jiang J, Ma J, Pang S, Liu Y, Yang Y, Luo C, Zhang J, Gu J, Qin W (2015) ABTS as an electron shuttle to enhance the oxidation kinetics of substituted phenols by aqueous permanganate. Environ Sci Technol 49:11764–11771

Steger PJ, Mühlebach SF (1997) In vitro oxidation of i.v. lipid emulsions in different all-in-one admixture bags assessed by an iodometric assay and gas-liquid chromatography. Nutrition 13:133–140

Sully BD, Williams PL (1962) The analysis of solutions of per-acids and hydrogen peroxide. Analyst 87:653–657

Tahirović A, Čopra A, Omanović-Mikličanin E, Kalcher K (2007) A chemiluminescence sensor for the determination of hydrogen peroxide. Talanta 72:1378–1385

Wang T, Reckhow DA (2016) Spectrophotometric method for determination of ozone residual in water using ABTS: 2.2′-Azino-bis(3-ethylbenzothiazoline-6-sulfonate). Ozone Sci Eng 38:373–381

Wang D, Zou J, Cai H, Huang Y, Li F, Cheng Q (2018) Effective degradation of Orange G and Rhodamine B by alkali-activated hydrogen peroxide: roles of HO_2^- and $O_2^{\cdot-}$. Environ Sci Pollut Res 221:117–124

Zhang K, Mao L, Cai R (2000) Stopped-flow spectrophotometric determination of hydrogen peroxide with hemoglobin as catalyst. Talanta 51:179–186

Zou J, Cai H, Wang D, Xiao J, Zhou Z, Yuan B (2019a) Spectrophotometric determination of trace hydrogen peroxide via the oxidative coloration of DPD using a Fenton system. Chemosphere 224:646–652

Zou J, Huang Y, Zhu L, Cui Z (2019b) Multi-wavelength spectrophotometric measurement of persulfates using 2,2′-azino-bis(3-ethylbenzothiazoline-6-sulfonate) (ABTS) as indicator. Spectrochim Acta A 216:214–220